Tree Physiology 19, 407–420

Canopy photosynthesis of sugar maple (*Acer saccharum*): comparing big-leaf and multilayer extrapolations of leaf-level measurements

FRÉDÉRIC RAULIER, PIERRE Y. BERNIER and CHHUN-HUOR UNG

Natural Resources Canada, Canadian Forest Service, Laurentian Forestry Centre, 1055 du P.E.P.S., P.O. Box 3800, Sainte-Foy, Québec, G1V 4C7, Canada

Received November 12, 1998

Summary A comparison is made between a big-leaf model (i.e., without details of the canopy profile) and two multilayer models (i.e., with details of the canopy profile) to estimate daily canopy photosynthesis of a sugar maple (*Acer saccharum* Marsh.) stand. The first multilayer model uses the distribution of leaf area by leaf mass per unit area (LMA) classes, the observed relationships between the parameters of a photosynthesis–irradiance curve and LMA, and the relationship between relative irradiance and LMA to estimate canopy photosynthesis. When compared with this model, the big-leaf model underestimates daily canopy photosynthesis by 26% because of an assumed proportionality between photosynthetic capacity and relative irradiance, a proportionality that is inconsistent with our data. The bias induced by this assumption is reduced when the big-leaf model is compared with the second multilayer model which, in addition to the assumptions made for the first multilayer model, accounts for the sunlit and shaded fractions of leaf area. The residual bias is almost eliminated when the big-leaf model is run using a weekly averaged irradiance. It is likely, however, that this is the result of a compensating bias that, in this particular case, compensates for the initial bias introduced by the proportionality assumption. It is also shown that canopy photosynthesis can be represented by spatially inexplicit multilayer models that use leaf mass per area as a covariable to describe leaf characteristics and environment. Such models represent an interesting alternative to the biased big-leaf approach.

Keywords: big-leaf model, leaf mass per area, multilayer model.

Introduction

Forest canopies are complex structures in which the capture of light by leaves varies simultaneously over time and space. Modeling of canopy-level photosynthesis in tolerant hardwoods is helped by strong relationships that develop between the average light environment of the leaf and particular leaf properties such as leaf mass per unit area (Goulet and Bellefleur 1986, St-Jacques et al. 1991), nitrogen content and photosynthetic rates (Ellsworth and Reich 1993, Reich et al. 1995).

Both big-leaf (i.e., without details of the canopy profile) and multilayer (i.e., with details of the canopy profile) models are used to estimate canopy net photosynthesis. Multilayer models are more flexible because profiles of multiple environmental variables can be incorporated into the calculation of photosynthesis (Leuning et al. 1995, Williams et al. 1996). However, their complexity is a major drawback in modeling productivity over large areas. In such cases, modelers usually fall back on a simpler big-leaf approach in which the canopy is either arbitrarily represented by a single leaf (Running and Coughlan 1988, Amthor et al. 1994, Lloyd et al. 1995) or by a synthetic expression resulting from the analytical integration of leaf photosynthesis over the canopy (Thornley and Johnson 1990, Sellers et al. 1992, Kull and Jarvis 1995, de Pury and Farquhar 1997). Only the second type of big-leaf model is considered here.

When considering photosynthesis at the canopy level, big-leaf models have tremendous conceptual appeal both because they can be parameterized with leaf-level photosynthetic measurements, and because they provide a tractable mathematical solution at the canopy level. Their development relies on the assumption that nitrogen content and photosynthetic capacity (on an area basis) should be distributed in strict proportion to irradiance within the canopy to maximize photosynthesis (Field 1983, Farquhar 1989) or as a result of acclimation to the prevailing light environment (Kull and Jarvis 1995, Hollinger 1996). As with the model of Kull and Jarvis (1995), the photosynthesis predictions made by the model of Sellers et al. (1992) are proportional to the photosynthesis of unshaded leaves at the top of the canopy. Although useful, such a result contradicts the more classical consideration that canopy photosynthesis response to irradiance should be more linear than that of a leaf (Ceulemans and Saugier 1991). Kull and Jarvis (1995) acknowledge that their approach would differ in assessing canopy photosynthesis but they raised the question of how much such a big-leaf model would differ from actual canopy photosynthesis on an appropriate time scale of a week or more.

The objective of this work was therefore to quantify the necessary biases incurred when using a big-leaf model. In order to do so, we compared predictions of canopy net photosynthesis on sugar maple (*Acer saccharum* Marsh.) made with a big-leaf model with those resulting from a more complete representation of the canopy in which leaf mass per area (LMA) was used to relate light response properties to leaf area distribution. This work forms an integral part of the ECOLEAP project, an effort dedicated to the modeling of forest productivity in Canada over large areas, but with a spatial resolution pertinent to forest management applications (Bernier et al. 1999).

Model development

Leaf photosynthesis model

Both the big-leaf and multilayer models developed below need a function to describe the photosynthetic light response curve. To settle the model comparison solely on the integration of leaf photosynthesis over the canopy and not on the advantage of incorporating leaf energy balance profile or on the specific choice of a leaf photosynthesis model, we chose the non-rectangular hyperbola of Hanson et al. (1987). Such a function gives excellent fits when considering photosynthesis at the current atmospheric CO_2 concentration (Ellsworth and Reich 1992, 1993, Liu et al. 1997) and its parameters all have a biological significance:

$$A_n = A_{max}\left[1 - \left(1 - \frac{R_d}{A_{max}}\right)^{1 - \frac{I_a}{I_c}}\right]. \tag{1}$$

Table 1 provides a summary of the symbols used in the text. Parameters A_{max}, R_d and I_c are adjusted parameters, and I_a is the irradiance (μmol (m^2 leaf)$^{-1}$ s^{-1}) in the photosynthetically active wavebands (PAR: 400–700 nm) incident on the leaf surface. Parameter A_{max} corresponds to the photosynthetic capacity (μmol (m^2 leaf)$^{-1}$ s^{-1}); i.e., to A_n at I_a above saturation. Parameter R_d corresponds to the respiration rate at $I_a = 0$ (μmol (m^2 leaf)$^{-1}$ s^{-1}). Parameter I_c is the irradiance at the compensation point (μmol (m^2 leaf)$^{-1}$ s^{-1}).

Big-leaf approach (BL)

The derivation of a big-leaf model requires the integration of Hanson's photosynthesis model over the canopy. As with the non-rectangular hyperbolas of Thornley and Johnson (1990, their Equation 10.2a; see Kull and Jarvis 1995) and Smith (1937, cited in Gates 1980), Hanson's non-rectangular hyperbola can be analytically integrated over the canopy if one first assumes that (Sellers et al. 1992, Kull and Jarvis 1995, Wang and Polglase 1995):

$$A_{max} = A_{max.0}\frac{\overline{H}}{\overline{H}_0}, \tag{2}$$

where $A_{max.0}$ is the photosynthetic capacity of the topmost unshaded leaves; $\overline{H}$ and $\overline{H}_0$ are time-averaged radiation values (e.g., mol (m^2 ground)$^{-1}$ day^{-1}), respectively, at the corresponding level where A_{max} is observed and at the top of the canopy. Kull and Jarvis (1995) assume that only photosynthetic capacity varies through the canopy, while the other model parameters are kept constant. However, for Hanson's model to be integrated through the canopy, dark respiration and irradiance at the compensation point need to be related to irradiance. Dark respiration rate has been found to be proportionally (Givnish 1988, Niinemets and Tenhunen 1997) or linearly related to photosynthetic capacity (Ceulemans and Saugier 1991). The general relationship may therefore be written as:

$$R_d = \beta_2 + \beta_3 A_{max}, \tag{3}$$

where β_2 and β_3 are two estimated parameters (refer to "Materials and methods" for the estimation method used). To make the integration possible within the big-leaf model, we need to assume that parameter β_2 of Equation 3 is null (Sellers et al.

Table 1. List of the main symbols used. Symbols referred to only once are defined in the text.

Symbol	Definition
A_{max}, $A_{max.0}$	Leaf photosynthetic capacity (μmol (m^2 leaf)$^{-1}$ s^{-1}). $A_{max.0}$ is the photosynthetic capacity of the topmost unshaded leaves.
A_c	Canopy net photosynthesis (μmol (m^2 ground)$^{-1}$ s^{-1}).
A_n	Leaf net photosynthesis (μmol (m^2 leaf)$^{-1}$ s^{-1}).
H, H_0	Daily PAR radiation (mol (m^2 ground)$^{-1}$ day^{-1}). H_0 is measured at the top of the canopy.
$\overline{H}$, $\overline{H}_0$	Daily PAR radiation averaged over the growing season. $\overline{H}_0$ is calculated for the top of the canopy.
I_c, I_{c0}	PAR irradiance at the compensation point (μmol (m^2 leaf)$^{-1}$ s^{-1}). I_{c0} is the irradiance at the compensation point of the topmost unshaded leaves.
I, I_0, $I_{0.b}$	PAR irradiance at the top of the canopy (μmol (m^2 ground)$^{-1}$ s^{-1}). I_0 is measured at the top of the canopy. $I_{0.b}$ is the direct irradiance at the top of the canopy.
$\overline{k}$	Extinction coefficient averaged for the growing season.
k_b, k_d	Extinction coefficients for the direct (b) and diffuse (d) irradiances.
L^*	Leaf area index (m^2 leaf (m^2 ground)$^{-1}$).
R_d, R_{d0}	Leaf dark respiration rate (μmol (m^2 leaf)$^{-1}$ s^{-1}). R_{d0} is the dark respiration rate for the topmost unshaded leaves.
α	Leaf photosynthetic quantum efficiency (Equations 4 and 14).
β_0, β_1, β_2, β_3	Parameters of the leaf photosynthetic model (Equations 3, 9 and 14).
v_i	Fraction of leaf area included in a given class i of LMA.
ρ_L	Leaf mass per unit area (g (m^2 leaf)$^{-1}$).

1992). A comparable relationship has also been used between dark respiration and a parameter describing Rubisco activity (Farquhar et al. 1980, Sellers et al. 1992).

One can also expect a strong proportionality between dark respiration rate and irradiance at the compensation point. The photosynthetic quantum efficiency α corresponds to the slope of the irradiance response curve when I_a tends to 0 (e.g., Thornley and Johnson 1990). Because R_d and I_c are found in the mostly linear part of the curve, the value of I_c can be estimated by the ratio:

$$I_c = -\frac{R_d}{\alpha}, \tag{4}$$

where the quantum efficiency, α, is a parameter to estimate. Here, we implicitly assume that α remains constant throughout the canopy (Thornley and Jonhson 1990, Ellsworth and Reich 1992).

Finally, we must assume that relative irradiance decreases with cumulative LAI (Monsi and Saeki 1953, Thornley and Johnson 1990, Sellers et al. 1992):

$$I = I_0 e^{-\bar{k}L^*}, \tag{5}$$

in which L^* is the stand LAI; I and I_0 are the irradiances in the photosynthetically active wavebands incident on a horizontal plane (µmol (m^2 ground)$^{-1}$ s^{-1}), respectively below the considered LAI and above the canopy; and $\bar{k}$ is an average light extinction coefficient. If we assume in the big-leaf model that $\bar{k}$ is constant and if we do not discern the diffuse and direct radiations, we can show from Equation 5 that the instantaneous relative irradiance at a point relative to that above the canopy is equal to the relative radiation integrated over a period of time:

$$\frac{I}{I_0} = \frac{\overline{H}}{\overline{H}_0}. \tag{6}$$

Equation 6 serves to relate Equations 2, 3 and 4 with Equation 1.

Canopy net photosynthesis A_c (µmol (m^2 ground)$^{-1}$ s^{-1}) is defined as (Thornley and Johnson 1990):

$$A_c = \int_0^{L^*} A_n \mathrm{d}L^*. \tag{7}$$

Noting that the irradiance absorbed by unit leaf area is the product of light extinction coefficient $\bar{k}$ and incident irradiance (e.g., Spitters 1986, Thornley and Johnson 1990, their Equation 8.6i), A_c is estimated by solving Equation 7:

$$A_c = A_{max.0}\left[1 - \left(1 - \frac{R_{d.0}}{A_{max.0}}\right)^{1 - \frac{\bar{k}I_0}{I_{c0}}}\right]\frac{1 - e^{-\bar{k}L^*}}{\bar{k}}, \tag{8}$$

where $R_{d.0}$ and $I_{c.0}$ correspond to dark respiration rate and irradiance at the compensation point for the topmost unshaded leaves, respectively.

First multilayer approach (ML-1)

Two important elements of the big-leaf model might lead to biased estimates of canopy photosynthesis. The first is the set of assumptions shown in Equations 2 to 6 and in particular the proportionality assumption of Equation 2 that make the analytical integration of Equation 1 possible. The second is the lack of differentiation between the direct and diffuse components of irradiance (Norman 1993, de Pury and Farquhar 1997). These are successively considered below in two multilayer models so that their relative effect on model outcome becomes apparent.

The first multilayer model is quite comparable to that of Reich et al. (1990). Instead of directly relating photosynthetic capacity to relative irradiance (Equation 2), a covariable such as leaf mass per area can be used. Ellsworth and Reich (1992, 1993) and Liu et al. (1997) have shown for sugar maple that a linear relationship can be expected between leaf mass per area and photosynthetic capacity:

$$A_{max} = \beta_0 + \beta_1\rho_L, \tag{9}$$

where ρ_L is the leaf mass per area (g (m^2 leaf)$^{-1}$) and β_0 and β_1 are two estimated parameters. With Equations 3, 4 and 9, all three parameters of Hanson's model are now indirectly related to leaf mass per area. If stand leaf area is stratified per LMA class and if the relationship between LMA and relative irradiance averaged over the growing season is known (Ellsworth and Reich 1992, Burton and Bazzaz 1995, Tjoelker et al. 1995), net photosynthesis can be estimated for the canopy, independently of the vertical distribution of leaf area in the canopy:

$$A_c = L^*\sum_i v_i A_n\{\bar{k}I\}, \tag{10}$$

where v_i is the fraction of leaf area included in a given class i of LMA and $A_n\{\bar{k}I\}$ is net photosynthesis (Equation 1) corresponding to an irradiance I estimated with Equation 5.

Second multilayer approach (ML-2)

The LMA is related to the time-averaged irradiance that impinges on it. However, at the scale of seconds or minutes, a fraction of the leaf area within any given LMA class will be illuminated by direct and diffuse irradiance, whereas the complementary fraction will be illuminated by diffuse irradiance only (penumbral effects are ignored). Because the relationship between leaf photosynthesis and irradiance is nonlinear, the use of mean irradiance (as in ML-1) will tend to overestimate photosynthesis (Spitters 1986, Norman 1993).

The time-averaged irradiance observed for a given LMA class can be used to approximate the LAI above the considered class (Equations 5 and 6). That LAI value can then be used with Equation 5 and an appropriate extinction coefficient to estimate the proportions of direct and diffuse irradiances reaching that LMA class, still without assessing any vertical distribution of leaf area. Canopy net photosynthesis can then be estimated as:

$$A_{\mathrm{c}} = L^{*}\sum_{i}\left[v_i\left(f_{\mathrm{b}.i}A_{\mathrm{n}}\left\{k_b I_{0.b} + k_d I_{\mathrm{d}}\right\} + (1 - f_{\mathrm{b}.i})A_{\mathrm{n}}\left\{k_d I_{\mathrm{d}}\right\}\right)\right], \quad (11)$$

where k_b and k_d are the extinction coefficients respectively for direct ($I_{0.\mathrm{b}}$) and diffuse (I_{d}) irradiances (μmol (m^2 ground)$^{-1}$ s^{-1}), $I_{0.\mathrm{b}}$ is the direct irradiance above the canopy, $f_{\mathrm{b}.i}$ corresponds to the fraction of sunlit leaf area for an LMA class *i* and equals the fraction of direct irradiance reaching the considered class (Spitters 1986, his Equation 19). Scattering of photosynthetically active radiation is not considered (Baldocchi 1993).

We therefore have three methods of estimating canopy net photosynthesis. The big-leaf model (BL) does not require details of the canopy profile and is obtained by analytically resolving the integral of leaf photosynthesis through the canopy (Equation 8). Multilayer models ML-1 and ML-2 are both based on numerical summation over the canopy (Equations 10 and 11). ML-1 (Equation 10) incorporates different assumptions (Equation 9 versus Equation 2) from those used by BL to relate leaf photosynthesis parameters to canopy properties, and ML-2 incorporates a separate treatment of direct and diffuse irradiance (ML-2, Equation 11).

Materials and methods

Study sites

We used field data collected in two stands of contrasting vertical structure and dominated by mature sugar maple in southern Québec to compare the three models (BL, ML-1 and ML-2) developed above. The St. Gilles site (46°26′30″ N, 71°25′00″ W) is located about 50 km south of Québec City, Canada on the St. Gilles de Beaurivage forest property of Daishowa, Inc. The site lies within the sugar maple–basswood–yellow birch climatic domain, ecological region 2c, of Thibault (1985), with degree-days above 5 °C of 166 to 178, and is underlain by a medium to fine sand deposit of alluvial origin. The stand is on relatively level ground, above poorly drained forested wetlands. It is composed primarily of sugar maple, with a small (10% of basal area) component of American beech (*Fagus grandifolia* Ehrh.) and yellow birch (*Betula alleghaniensis* Britt.) and originates from a complete cut dating from the 1930s. The stand is mostly even-aged and forms a closed, homogeneous canopy with few gaps. Dominant and codominant tree heights range from about 22 to 27 m. Live crown depth is about 5 m. Maple regeneration forms a nearly continuous single-leaf cover at a height of about 50 cm.

The Duchesnay site (46°56′36″ N, 71°40′00″ W) is located within the bounds of the Duchesnay Forest Station, managed by the Québec Ministry of Natural Resources. The site lies within the sugar maple–yellow birch climatic domain, ecological region 3g, of Thibault (1985), with degree-days above 5 °C of 122 to 155, and is underlain by a coarse and bouldery granitic basal till. The site has a 15% south-facing slope. Sugar maple accounts for about 74% of the basal area, with yellow birch and American beech accounting for 18 and 8% of the basal area, respectively. The stand was subjected to repeated highgrading until its acquisition by the Province of Québec in the late 1950s. From that point on, new gaps were left to regenerate naturally where older trees fell. As a result, the stand is strongly uneven-aged. Dominant and codominant tree heights are about 25 m, but there are numerous trees of all height classes, and live foliage at all levels within the stand.

In the summer of 1996, a 25-m canopy access tower was erected at the St. Gilles site to permit the measurement of leaf gas exchanges in canopies of two adjacent sugar maple trees (A site). A meteorological tower was also put in place and instrumented with various sensors to monitor above and below canopy environmental variables. Incident shortwave radiation was measured above the canopy with silicon pyranometers (Model LI200S, Li-Cor, Inc., Lincoln, NE). Other environmental sensors were mounted on or around the towers. All sensors were scanned every minute. The hourly mean of their readings was recorded on a data logger.

For the present study, data from the St. Gilles site provided estimates of canopy photosynthesis, whereas the Duchesnay site was used to evaluate the variability of the distribution of leaf area per LMA class.

Leaf gas exchange

Leaf gas exchange measurements were performed at the St. Gilles site only, on 5 days between July 8 and September 19, during the summer of 1997. Light response measurements were carried out *in situ* on attached leaves with a portable gas exchange measurement system (Model LCA4, Analytical Development Corp., Hoddesdon, U.K.) working in an open mode, and equipped with a broad leaf cuvette with the capability for climate control. Cuvette and leaf temperatures were monitored with built-in sensors and energy balance corrections. Photosynthetically active radiation (PAR) was monitored during all measurements with a quantum sensor mounted directly on the cuvette handle. All irradiance measurements reported are for PAR wavelengths.

Depending on irradiance conditions or on the type of leaves selected, light response measurements were performed with natural or artificial light. Under sunny skies (incident irradiance above 1000 μmol m^{-2} s^{-1}), when working on leaves at or near the canopy top, measurements were done with direct sunlight. Lower irradiances required in generating the light response curves were obtained with three large neutral density filters of different opacity. Depending on the available irradiance, the filters were combined to obtain at least five points on each response curve, including saturation (above 1200 μmol m^{-2} s^{-1}) and total darkness (0 μmol m^{-2} s^{-1}). Target irradiances for the three intermediate points were at or near points of physiological interest according to the recommendations of Hanson et al. (1987). We usually aimed for irradiance at the compensation point, a point in the steepest portion of the light response curve, and one point nearer to the zone of curvature. The actual target values changed with the type of leaves measured within the canopy.

On overcast days, or when working on shade leaves exposed only to transient sunflecks, we used the artificial light source provided by ADC to generate appropriate irradiances. The light source consists of a white halogen bulb and reflector mounted directly on the cuvette. Air gaps and thermal filters prevented heat build-up in the cuvette. Irradiance was controlled through the use of a built-in voltage regulator, coupled with a diffusor and small neutral-density filters. Irradiance in the cuvette was measured before each measurement with a small detachable quantum meter. Irradiance targets were similar to those used with natural light.

On each sampling day, light response curves were obtained on three to seven leaves. These leaves were selected from three canopy positions: direct sun exposure at the top of the crown, an intermediate canopy position, and either the base of the living crown or the maple regeneration layer on the forest floor. All measurements were carried out between 1000 and 1500 h. A total of 24 response curves were obtained during the summer.

After the measurements were completed, the leaves were tagged, detached, placed in a leaf press and left to dry. In late September, after the last field measurements, we scanned each leaf (Scanjet IIcx/T, Hewlett Packard, Minneapolis, MN) and obtained its area, excluding any interior holes, to the nearest 0.1 mm^2 with image analysis software (NIH Image v1.61, National Institutes of Health, Bethesda, MD). Dry mass of each leaf was determined thereafter to the nearest 0.1 mg. Leaf mass per area (LMA) was computed for individual leaves as the ratio of dry mass to leaf area (g m^{-2}). All measurements excluded the petiole.

Equation 1 was parameterized in three steps. We first fitted Equation 1 to data from individual leaves. The nonlinear ordinary least-square (OLS) fit of the function to the data was done with the PROC NLIN procedure available with the SAS statistical software package (SAS Institute, Cary, NC). In a second step, using the results from the 24 fitted functions, we related the estimated parameters of Hanson's model ($A_{\max}$, R_d and I_c) to values of leaf mass per area as per Equations 3, 4 and 9, thus obtaining estimates of the different parameters used in these equations. Finally, the $A_{\max}$, R_d and I_c parameters in Equation 1 were replaced with their respective parameterized equations, and the full model estimated once more with nonlinear OLS (West et al. 1984).

For the big-leaf model, it is necessary to assume that parameter α_2 in Equation 3 is equal to zero. A likelihood ratio (Bates and Watts 1988) was used to test the significance of the parameter.

Leaf area and leaf mass per area measurements

Destructive measurements of total canopy leaf area, and of the LMA distribution within the canopy were made at both the St. Gilles and Duchesnay sites. At St. Gilles, because of the homogeneity of the stand, all destructive measurements were carried out within a single 1000-m^2 circular plot located sufficiently away from the canopy-access tower to prevent any influence on other longer term measurements around the canopy-access and meteorological towers. At Duchesnay, sampling took place in three 1000-m^2 plots to capture the variability of the stand, but results from only two plots are considered here because the third plot was dominated by yellow birch.

Within each plot targeted for destructive measurements, we measured tree height, diameter at breast height and social class of all trees. Social classes were: dominant and codominant (one class), intermediate and suppressed. For sugar maple, two or three trees from each of these three classes were selected and felled for destructive determination of total leaf mass and area. For yellow birch and American beech, trees were also selected and felled in numbers related to their relative contribution to total basal area.

The method used to estimate leaf area is detailed in Raulier and Ung (1997). The diameter of each second-order live branch was measured to the nearest millimeter at one diameter from its point of insertion on the stem. The crown was then separated into two portions, the light crown and the shade crown, above and below the level of greatest crown width (Burger 1939). Two branches were selected within each part for further analysis using a selection process based on the cross-sectional area of the branch at its insertion point. This method links the probability of selection to the cross-sectional area of the branch at the point of insertion, which is itself considered proportional to the leaf area supported by the branch according to the pipe model theory of Shinozaki et al. (1964). The Randomized Branch Sampling method (RBS; Gregoire et al. 1995) was then applied twice within each branch for leaf sampling. With RBS, each branch can be considered as a network of segments and nodes through which one can trace a path. Starting at the base of the branch, the selection at each node of the segment to follow was performed randomly according to the basal area of the respective segments starting at the node. On each selected segment, we counted all short shoots (the short leaf-carrying segments that grow out of second- or third-order segments; Powell et al. 1982). Finally, we sampled all leaves from one short shoot and the terminal long shoot on each of the two sampled paths. The area and dry mass of all leaves collected through RBS sampling were measured at the laboratory and served to estimate a mean short- and long-shoot leaf area and mass per branch.

The scaling up from the leaf samples to the tree was done by working backward from the branch's tip down individual paths, and incrementally adding leaf area from short shoots and from the other unselected segments at each node, based on their cross section relative to that of the selected path at that node. For each part of the crown, leaf area was estimated as the product of the sum of leaf area measured on the selected branches and the ratio between the sum of the branch basal areas of the crown part and that of the selected branches. These leaf areas for each crown part were then summed to obtain the leaf area of the tree.

To estimate leaf area index at the stand level (A and B sites), we proceeded differently for sugar maple than for yellow birch and American beech. For sugar maple, a sufficient number of sampled trees allowed us to estimate the following relationship between leaf area and diameter at breast height (DBH, cm):

$$L = \lambda_1 d_{1.3}^{\lambda_2}, \tag{12}$$

where L is the leaf area of a tree (m^2), $d_{1.3}$ is the diameter at 1.3 m (cm) and λ_1 and λ_2 are estimated parameters. Heteroscedasticity was modeled assuming a multiplicative residual error. Logarithmic transformation was therefore applied to Equation 12 and the log bias was corrected when returning to the original units of measurement (Baskerville 1972). For yellow birch and American beech, leaf area measurements made by Denis Ouellet (unpublished data) sampled at the Duchesnay forest station were used to estimate the parameters of Equation 12. The sampling procedure is identical to that described by Ouellet (1995) for sugar maple. A paired *t*-test was then used on the residuals at the logarithmic scale to test the departure of leaf areas estimated in the B sites for both species from their respective equations. Leaf area index was then calculated by estimating the leaf area of all the trees from their respective DBH.

To estimate the distribution of leaf area per LMA class, we first estimated the frequency at the stand level that each collected leaf would represent on the B sites. The frequency v represented by a single sampled leaf was calculated as:

$$v_{lbcts} = L^c_{lbcts} \frac{L_{bcts} A_{cts} G_s}{L^c_{bcts} A^c_{cts} G^c_s} \frac{1}{L_\mathrm{p}},$$

where subscripts l, b, c, t and s represent a leaf l on a branch b selected in crown portion c of a tree t in social class s. Superscript c indicates a collected sample. Variable L is leaf area (m^2), A is the sum of branch basal areas (cm^2), G is basal area at the plot level (m^2 ha^{-1}) and L_p is the plot total leaf area. Each collected leaf was classified into LMA classes of 20 g m^{-2} amplitude. The relative frequency v_i of leaf area for a given LMA class defined by lower and upper bounds b_l and b_u, in a given plot, is equal to:

$$v_\mathrm{i} = \sum_s \sum_t \sum_c \sum_b \sum_l \begin{cases} v_{lbcts} & \text{if } \rho_{L.lbcts} \in [b_\mathrm{l}, b_\mathrm{u}[\\ 0 & \text{otherwise} \end{cases}.$$

A simple mathematical mean was calculated between the respective plots of each site to scale at the stand level.

Relationship between leaf mass per area and irradiance

Ellsworth and Reich (1993, their Figures 1 and 4a), Tjoelker et al. (1995, their Figure 6b), Burton and Bazzaz (1995, their Figures 7 and Table 1) and Ellsworth (Brookhaven National Laboratory, Upton, NY, unpublished data) used incident irradiance on predominantly sunny days averaged over the growing season to characterize and compare irradiance environments among sugar maple branches, leaves or relative positions of leaves in the canopy. Except for Tjoelker et al. (1995), the other above-cited references gave sufficient information to estimate the relationship between LMA and relative irradiance. For the data of Tjoelker et al. (1995), we divided the average irradiance by an estimated PAR irradiance above the canopy of 35 mol m^{-2} day^{-1}, equivalent to that measured by Ellsworth and Reich (1992, their Table 1) for a comparable location and predominantly sunny conditions in a clearing. A preliminary examination of the relationship between LMA and relative irradiance showed that it could be modeled with a logistic relationship (e.g., Ratkowsky 1990):

$$\frac{\overline{H}}{\overline{H}_0} = \frac{1}{1 + \exp(-\mu_1(\rho_\mathrm{L} - \mu_2))}, \qquad (13)$$

where μ_1 and μ_2 are two parameters estimated with OLS.

We validated Equation 13 for our field sites with LMA distribution data. Because LMA is a monotonically decreasing function of LAI (e.g., Jurik 1986, Ellsworth and Reich 1993), leaf area of the classes of greater LMA can be cumulated to estimate a cumulated shading LAI. With Equations 5 and 6, this shading LAI allows one to estimate the relative irradiance experienced by the leaves within any given LMA class.

Extinction coefficients

The BL and ML-1 models require a single average extinction coefficient because they both use Equation 5 to describe the relationship between LAI and average irradiance. Model ML-2, on the other hand, requires separate extinction coefficients for the diffuse and direct portions of the solar irradiance. The mean extinction coefficient of Equation 5 was numerically estimated, accounting both for diffuse and direct components of irradiance and for the range of solar angles encountered during the growing season (Appendix). Because most of the data used to estimate the parameters of Equation 13 were measured under predominantly sunny conditions, the calculations were repeated with a fixed proportion of diffuse irradiance of 15% (e.g., Gates 1980, Spitters et al. 1986) instead of one that varies as a function of weather. For the second multilayer approach (ML-2), the proportion of diffuse and direct components of irradiance and sun elevation was estimated with the same procedures as those used for the calculation of the averaged extinction coefficient (Appendix).

Canopy photosynthesis

The three models (BL, ML-1 and ML-2) were first used to estimate hourly canopy net photosynthesis at the St. Gilles site from May 15 to September 15, 1997. Only irradiance was allowed to fluctuate. All other environmental conditions were considered to be optimal. The incident shortwave radiation measured above the canopy of the St. Gilles site was used to drive the simulations. The PAR irradiance was computed as half the shortwave irradiance (Ross 1975, Aber et al. 1996). For the big-leaf model, neither Sellers et al. (1992) nor Kull and Jarvis (1995) give an objective and practical definition of the topmost unshaded leaves. We used a relative irradiance of 95% as the mean for topmost leaves, and used Equations 13, 3, 4 and 9 to derive their photosynthetic characteristics.

Hourly estimates obtained with the three models were cumulated into daily and weekly totals for comparisons. Weekly canopy photosynthesis was also estimated with the big-leaf model using the weekly averaged irradiance (week-BL).

Results and discussion

Leaf gas exchange measurements

Photosynthetic capacity varied from about 12 μmol m^{-2} s^{-1} for sun leaves at the top of the canopy to 3.5 μmol m^{-2} s^{-1} for leaves either at the base of the live crown or in the regeneration layer. These values were very consistent within each of these two extreme canopy positions. We did not observe midday stomatal closure or photosynthetic depression in our trees, possibly because none of the sampling days presented particularly hot and dry conditions. Also, we intentionally spread the measurements across most of the growing season in order to capture late season phenological effects. The A_{max} values obtained on September 19, just days before hard frosts and the onset of fall senescence, were identical to those measured throughout the summer. All light response curves of the different sampling days were therefore lumped for the remainder of the analysis.

The fits of Equation 1 to the photosynthetic light response of individual leaves were excellent, with nearly all R^2-values above 0.95. This goodness of fit was expected, given the applicability of the model for this particular shape of curve, and the fact that each curve was based on only five data points for the three-parameter model. The response curves for full sun and deep shade leaves were predictably different. Overall, shade leaves had a much lower photosynthetic capacity than sun leaves (about 3.5 versus 12 μmol m^{-2} s^{-1}), saturated at lower irradiances (as low as 100 versus 1000 μmol m^{-2} s^{-1}), and had a lower irradiance at the compensation point (10 versus 40 μmol m^{-2} s^{-1}). Respiration rates were also related to the canopy position of the leaves, with shade leaves having lower respiration rates (about −0.3 μmol m^{-2} s^{-1}) than sun leaves (about −1.0 μmol m^{-2} s^{-1}). All these differences are consistent with the known morphological and physiological differences between sun and shade leaves in sugar maple (Hagen and Chabot 1986, Ellsworth and Reich 1993).

The second step in the procedure was to express the three parameters (A_{max}, R_d and I_c) of the light response curves (Equations 3, 4 and 9) as a function of LMA. Simple linear relationships (Equations 3, 4 and 9) seemed adequate in all cases (Figure 1). Equation 1 was reestimated with the parameterized relationships included in the model (Equations 3, 4 and 9). With a likelihood ratio test, parameter β_0 of Equation 9 was not significantly different from zero (F_{obs} = 0.22, $F_{(0.05;1;121)}$ = 3.92). The final parameterized version of Equation 1 estimated with nonlinear OLS is then:

$$A_n = A_{max}\left[1 - \left(1 - \frac{R_d}{A_{max}}\right)^{1 - \frac{I_a}{I_c}}\right]$$

$$\text{where } A_{max} = \beta_1 \rho_L,$$
$$R_d = \beta_2 + \beta_3 A_{max},$$
$$I_c = -R_d/\alpha, \qquad (14)$$

where the values of the different parameters are listed in Table 2. The assumption needed for the big-leaf photosynthesis model (parameter β_2 of Equation 14 being equal to zero, Table 2, Equation 14′) was significantly rejected with a likelihood ratio test (F_{obs} = 4.41, $F_{(0.05;1;121)}$ = 3.92). Despite this result, the mean square errors and determination coefficients of Equations 14 and 14′ were only slightly different (Table 2). An analysis of the residuals of Equation 14 showed no apparent trend with any of the variables examined (Figure 2).

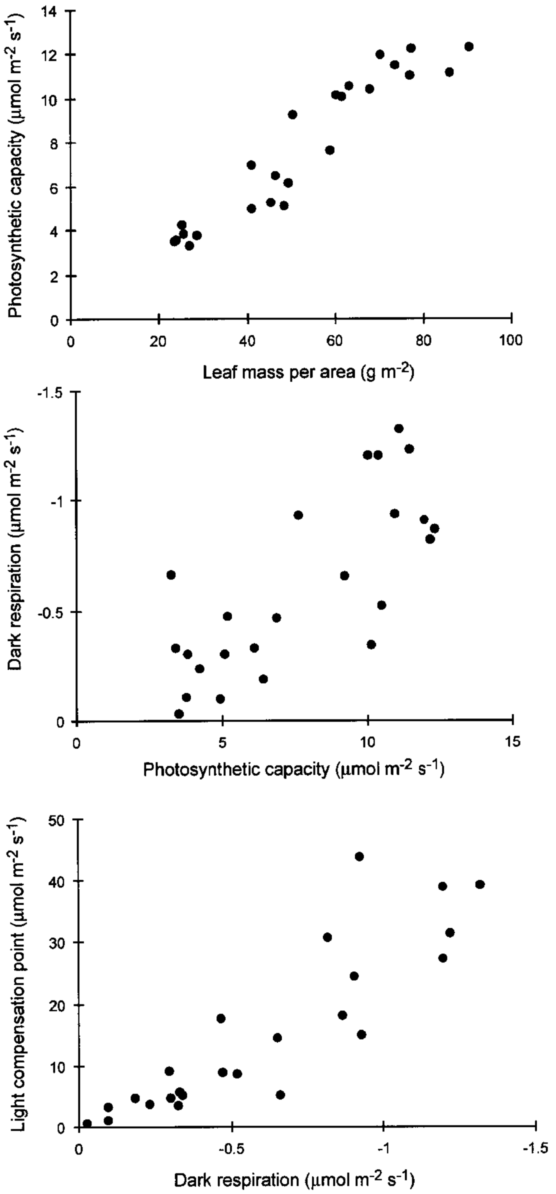

Figure 1. Observed relationships between the three model parameters of Hanson et al. (1987) (Equation 1) estimated from the leaf gas exchange measurements on 24 leaves at the St. Gilles site and leaf mass per area (Equations 3, 4 and 9). Note that dark respiration is expressed on a negative scale.

Ellsworth and Reich (1993) have shown that, for sugar maple, variation of nitrogen on an area basis is a direct consequence of vertical variation of leaf mass per area. They have also shown that nitrogen on an area basis is linearly related to LMA. Nitrogen and consequently the parameters of a photosynthesis model, when expressed on a mass basis, should thus

Table 2. Model statistics. Number of observations (n), mean square error (MSE), adjusted coefficient of determination (R^2_{adj}), parameter estimates, standard error (SE) and correlation matrix. Abbreviations: SM, YB and AB correspond to sugar maple, yellow birch and American beech, respectively.

Model	n	MSE	R^2_{adj}	Parameters					
				Estimated value		SE	Correlation matrix		
Equation 12 (SM)	27	0.3073[1]	0.734[1]	λ_1	−0.271[2]	0.588	1		
				λ_2	1.639	0.192	−0.98	1	
Equation 12 (YB)	35	0.0536[1]	0.964[1]	λ_1	−0.543[2]	0.172	1		
				λ_2	1.801	0.060	−0.97	1	
Equation 12 (AB)	15	0.0726[1]	0.898[1]	λ_1	0.795[2]	0.352	1		
				λ_1	1.294	0.116	−0.98	1	
Equation 13	56	0.0110	0.893	μ_1	0.078	0.007	1		
				μ_2	70.069	1.464	−0.47	1	
Equation 14	125	0.9487	0.917	β_1	0.145	0.004	1		
				β_2	0.168	0.049	−0.20	1	
				β_3	0.809	0.393	−0.06	0.89	1
				α	0.041	0.003	−0.43	0.38	0.06
Equation 14′[3]	125	0.9752	0.914	β_1	0.145	0.004	1		
				β_3	0.080	0.022	−0.25	1	
				α	0.041	0.003	−0.43	0.69	1

[1] Given on the logarithmic scale.

[2] Constant estimates given on the logarithmic scale. Includes the correction accounting for the bias induced by the logarithmic transformation.

[3] Equation 14é is Equation 14 with parameter β_2 set to zero.

remain more or less constant through the canopy (Ellsworth and Reich 1993, Harley and Baldocchi 1995, Hollinger 1996). This is the case with our data, because the photosynthetic capacity expressed on an area basis is proportional to LMA (Equation 14) and the other parameters of Hanson's photosynthesis model are related to $A_{\max}$ (Equations 3 and 4). Leaf mass per area is much easier to measure than nitrogen concentration, but the relationships between LMA and leaf photosynthesis parameters remain, at most, species specific (Kull and Jarvis 1995, Reich et al. 1995).

Leaf area, leaf mass per area and relative irradiance

Estimated leaf area indices were 8.45 and 9.28 (single sided) for the St. Gilles and Duchesnay stands, respectively. The estimated relationship between leaf area and DBH for sugar maple (Equation 12, Table 2) was comparable to those of Burton et al. (1991) and Ouellet (1995). Burton et al. (1991) also estimated similar LAI values with an allometric method for stands of comparable DBH sizes and basal areas (25.3 cm and 28.9 m^2 ha^{-1} for St. Gilles and 20.4 cm and 30.7 m^2 ha^{-1} for Duchesnay).

The relative distributions of leaf area per LMA class were similar for both stands (Figure 3a): a mean LMA of 56.0 and 60.3 g m^{-2} with a standard deviation of 22.1 and 22.3 g m^{-2} for St. Gilles and Duchesnay, respectively, with a strong skew toward the left (log-normal distributions). In both cases, approximately 70% of leaf area had an LMA between 30 and 70 g m^{-2}. The number of leaves that served to establish these distributions was 486 and 1377 leaves for St. Gilles and Duchesnay, respectively.

Estimates of $\bar{k}$ based on variable proportions of direct and diffuse radiations yielded values of 0.50 for both stands. Similar values of $\bar{k}$ were obtained for both stands using a fixed (15%) diffuse proportion of total irradiance. Based on this value, the relationship between relative irradiance and LMA computed with Equations 5 and $\bar{k}$ compares well with the data of Ellsworth and Reich (1993), Tjoelker et al. (1995), Burton and Bazzaz (1995) and Ellsworth (unpublished data) (Figure 4), although our estimate of $\bar{k}$ takes into account an estimate of direct and diffuse radiation, whereas their data are measurements obtained on predominantly sunny days (low and fixed diffuse component). This similarity underlines the low sensitivity of the estimated extinction coefficients at these high LAIs to discrimination of sun angle or irradiance components.

Canopy photosynthesis

As expected, neither multilayer model (ML-1 and ML-2) saturated with increasing irradiance as quickly as the big-leaf model (BL) (Figure 5a). On average, when compared with ML-1, BL underestimated daily canopy photosynthesis by 0.27 mol m^{-2} day^{-1} (± 0.18 SD). This bias represents 26% of mean ML-1 canopy photosynthesis on the daily and weekly scales. The BL and ML-1 differ in two respects; namely, the restrictive assumptions (particularly Equation 2) required for the analytical solvability of the big-leaf model and the inclusion of the distribution of leaf area by LMA class in ML-1.

To separate these two possible sources of difference, we produced a new big-leaf model in which the relationships between irradiance and $A_{\max}$ were described by Equation 9 instead of Equation 2. Equation 13, which relates LMA and relative irradiance, was then used to solve the integral of photosynthesis through the canopy (Equation 7). This change forced us to perform a numerical integration over the canopy,

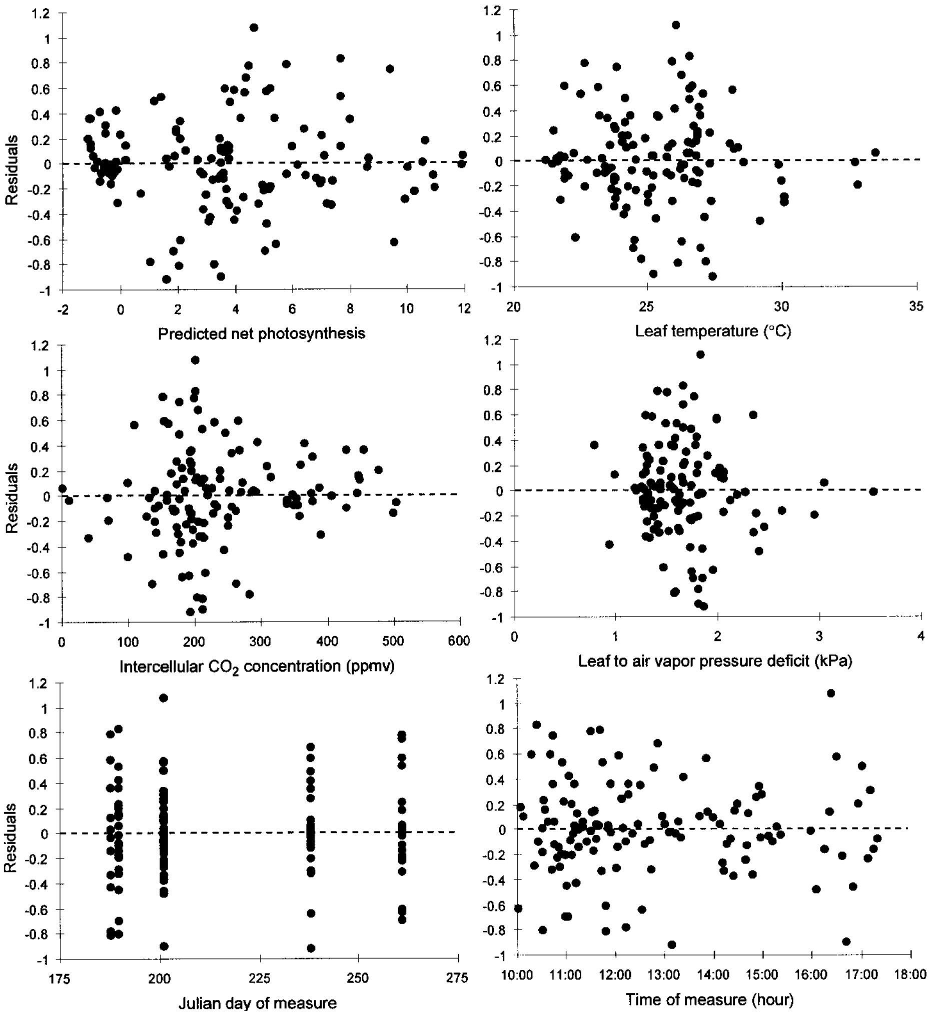

Figure 2. Residuals of Equation 19 versus predicted net photosynthesis, leaf temperature, intercellular CO_2 concentration, leaf to air vapor pressure deficit, Julian day of measure, and time of measure. These variables were observed during the measurements of leaf gas exchange made on 24 leaves at the St. Gilles site, which were used to calibrate Equation 14.

but the resulting bias fell to 0.03 mol m^{-2} day^{-1} (± 0.02 SD). In addition, the result was only slightly different whether the β_2 parameter of Equation 3 was considered to be null, or not. This result shows that the proportionality assumption between relative irradiance and photosynthetic capacity (Equation 2) used in big-leaf models (e.g., Sellers et al. 1992, Kull and Jarvis 1995) is incorrect. Combining Equations 9 and 13 shows that the relationship between photosynthetic capacity and relative irradiance is not proportional (Figure 6). This result is similar to that of Hollinger (1996) who showed that, in *Nothofagus fusca* (Hook. f.) Ørst., nitrogen concentration expressed on an area basis is not proportional to relative irradiance. Dang et al. (1997) have also shown that this proportionality assumption causes underestimation of canopy photosynthesis for black spruce (*Picea mariana* (Mill.) B.S.P.), aspen (*Populus tremuloides* Michx.) and jack pine (*Pinus banksiana* Lamb.) stands.

It is known that the use of averaged irradiance will cause a strong overestimation of canopy photosynthesis (e.g., Spitters 1986, Norman 1993, Landsberg and Gower 1997). Estimates of canopy photosynthesis with ML-1, a model that uses average irradiance, are therefore larger than those obtained with ML-2, a model that explicitly separates the direct and diffuse components of irradiance. However, neglecting the other factors limiting photosynthesis, neither ML-1 nor ML-2 correctly estimates canopy photosynthesis, but rather represents the upper and lower bound of the real value (Norman 1980). In real canopies, a fraction of the irradiance reaching the lower portions of the canopy comes as a penumbra, a region of partial shade, where only a portion of the sun disk can be seen. Simulation of penumbra requires a much more complicated description of canopy structure, especially leaf angle distribution and vertical distribution of leaf area (Denholm 1981). However, according to Norman and Jarvis (1975), the real effect of penumbra is likely to be small. The mean difference between ML-1 and ML-2 approximates 16% of the mean photosynthesis estimated with ML-1, on either daily or weekly scales. As noted by Norman (1980), this represents a maximum enhancement by penumbral effects and these effects are likely to be much less than 16%.

As noted above, we also produced weekly estimates of canopy photosynthesis by using a single value of weekly average irradiance with the BL model. Interestingly, the values obtained with this approach were quite comparable with those

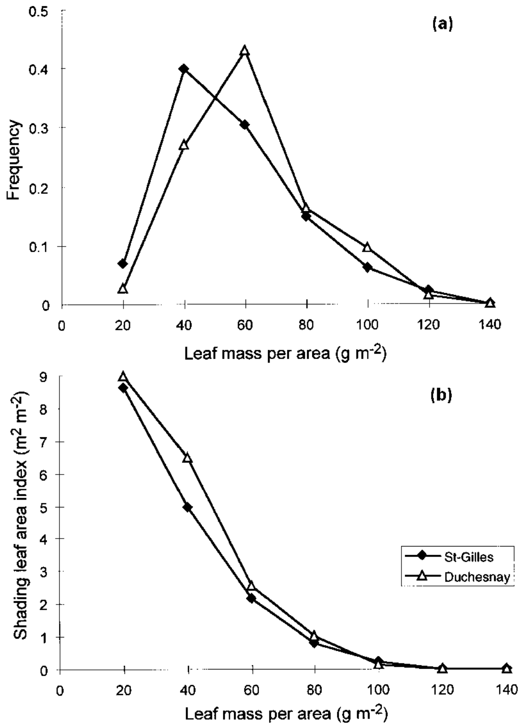

Figure 3. Observed distribution of leaf area per LMA class at the St. Gilles and Duchesnay sites (a). Leaf area of the classes of greater LMA were cumulated to estimate a cumulated shading LAI (b).

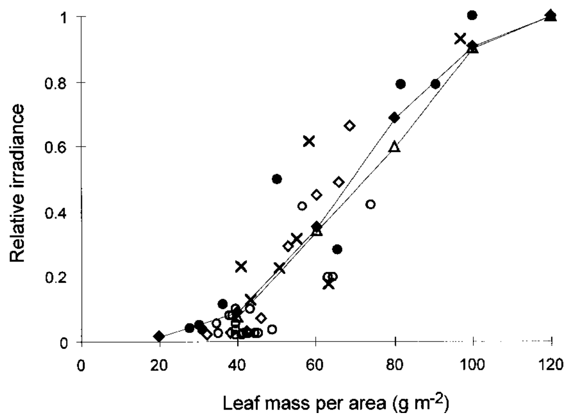

Figure 4. Observed relationship between leaf mass per area and relative irradiance (○: Tjoelker et al. 1995; ×: Burton and Bazzaz 1995; ◇: Ellsworth and Reich 1993; ●: Ellsworth, unpublished data; △: Duchesnay site; ◆: St. Gilles site).

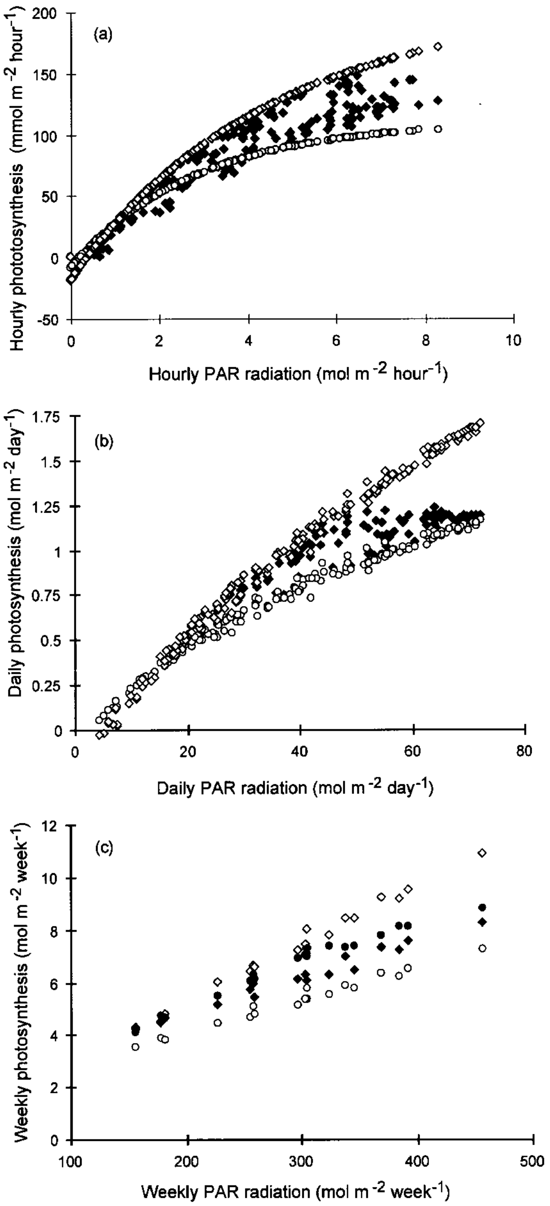

Figure 5. Predicted net canopy photosynthesis at the scale of hours (a), days (b) and weeks (c) (○: big-leaf model (BL); ●: weekly big-leaf model; ◇: multilayer model (ML-1); ◆: multilayer model (ML-2)).

obtained from the more complex ML-2 model (Figure 5c). We know from the previous comparisons that weekly estimates of canopy photosynthesis produced by the cumulated hourly estimates made with the BL model are severely biased downward compared with results from the ML-2 model (Figure 5c). It is obvious that using weekly average values of irradiance produces a compensating bias, which, in this particular case, results in a close fit with the more realistic representation. However, no assurance can be given that this compensation of biases will hold if the stand conditions, especially LAI, are changed.

The most important cause of negative bias observed with BL is the assumed proportionality between photosynthetic capacity and relative irradiance (Equation 2). A detailed analysis of the importance of assuming such a proportionality shows that it is the only option to find a simple analytical solution to the integral of at least three popular non-rectangular hyperbolas. For example, the non-rectangular hyperbolas of Smith (1937, cited in Gates 1980) and Thornley and Johnson (1990) are alternatively used to calculate the electron transport rate in the many different versions of the photosynthesis model defined

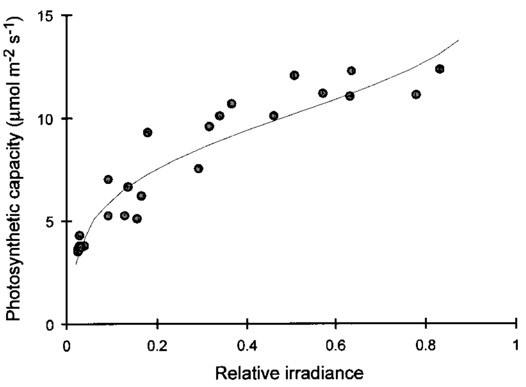

Figure 6. Predicted relationship between relative irradiance and photosynthetic capacity. The full circles represent the 24 leaves used for leaf gas exchange measurements at the St. Gilles site, for which the relative irradiance was estimated from their respective LMA with Equation 13. The line was predicted by varying LMA from 20 to 100 g m^{-2}, estimating relative irradiance from LMA with Equation 13 and photosynthetic capacity with Equation 9.

by Farquhar et al. (1980) (Harley et al. 1992, McMurtrie et al. 1992*a*, Bonan 1993, McMurtrie and Wang 1993, Wullschleger 1993, Harley and Baldocchi 1995). One important exception is a variant proposed by Collatz et al. (1991), which was used by Sellers et al. (1992). The last model does not use a non-rectangular hyperbola, and could be modified to include at least a linear relationship between photosynthetic capacity and relative irradiance. However, the integral of leaf photosynthesis through the canopy cannot be resolved anymore if a more complex relationship is used, such as the combination of Equations 9 and 13 proposed here. De Pury and Farquhar (1997) also propose a modified big-leaf model that does not require the above-mentioned proportionality and includes the differentiation between sunlit and shaded fractions of leaf area.

Spatially inexplicit multilayer models

Big-leaf models have a clear advantage over multilayer canopy models that require an explicit description of the vertical distribution of leaf area, such as those of Reich et al. (1990), Baldocchi (1993), Ellsworth and Reich (1993), Norman (1993), Baldocchi and Harley (1995), and of Williams et al. (1996). The vertical distribution of leaves required by these models is difficult and costly to obtain for forest stands, and prevents the extrapolation of the models to stands of the same species but with a different vertical structure (*sensu* O'Hara and Milner 1994). However, the multilayer models presented in this study and by other researchers (Leuning et al. 1995, Wang and Polglase 1995, de Pury and Farquhar 1997) do not require such a description because they are based on cumulative leaf area. These models retain the advantages of the explicit multilayer models because a leaf energy profile can still be included (Leuning et al. 1995). Height appears at first as a convenient variable to stratify the canopy leaf area but it is not a primary driving factor for local variability in leaf characteristics or leaf environment. Preliminary sampling at the St. Gilles site showed that the strongest gradients in the maximum rate of photosynthesis occurred near the top of the canopy and were more or less perpendicular to the exposed convoluted surface formed by the leaves of individual branches. Using a height-independent representation of canopy structure greatly improves the scaling up of the model from the plot to the stand and to groups of stands with different vertical canopy structures. As seen in the present study (Figure 3), two stands of different vertical structure but of similar LAIs had a comparable distribution of leaf area per LMA class.

The last intrinsic difference between a big-leaf and such spatially inexplicit multilayer models is the availability of an analytical solution at the canopy level for the big-leaf model, whereas the multilayer model requires a numerical solution. A criterion of choice could be the greater speed of calculation for the analytical solution. However, such a difference is strongly attenuated by the use of Gaussian integration, which requires the estimation of only three to five points (Leuning et al. 1995, Wang and Polglase 1995, de Pury and Farquhar 1997).

Finally, a major disadvantage of the big-leaf model is the difficulty of finding a field analog for the rigorous definition of the topmost unshaded leaves. The topmost unshaded leaf is a theoretical concept resulting from the analytical integration of leaf photosynthesis through the canopy (Equation 7). With the definition used in this paper (LMA corresponding to 95% of the irradiance above the canopy), the mean LMA of this leaf class is estimated as 108 g m^{-2}, which is particularly high for sugar maple. For the destructive plots at St. Gilles and Duchesnay where important leaf samples were taken, this LMA corresponds to a mean value of 5.9% of leaf area, when sorted by ascending LMA. It should be noted, however, that none of the leaves that were used for the gas exchange measurements (a much smaller sample size) at the St. Gilles site had such a high LMA value (Figure 1a), despite the fact that some leaves were sampled at the top of the canopy around the access tower. The parameters of the leaf photosynthesis model for these high values of LMA are therefore extrapolated beyond the actual measurements.

Other alternatives to the big-leaf model exist if the objective is to reduce the number of parameters required to describe canopy-level processes. Canopy relationships become linear on a weekly scale, independently of the assumptions used (Figure 5c). It seems possible therefore to calibrate for weekly or greater time steps, a model simpler than the big-leaf model, on the basis of simulations done with a finer, spatially inexplicit multilayer model. As suggested by Leuning et al. (1995), this approach can be used for the calibration of a light use efficiency model (McMurtrie et al. 1992*b*, Landsberg et al. 1996).

Conclusion

The objective of the present study was to assess how much a big-leaf model would differ from more complex multilayer models in predicting canopy net photosynthesis. Results show that the bias incurred by the use of a big-leaf model is between 15 and 26% compared with more complex multilayer models. Part of the difference between the models is due to the inadequacy of the assumptions needed in the big-leaf model to solve the integral of leaf photosynthesis through the canopy. In particular, the proportionality between photosynthetic capacity and relative irradiance needed by the big-leaf model is not correct according to our data. For a stand with a high LAI, the bias is attenuated when the big-leaf model is compared with a model that accounts for the sunlit and shaded fractions of leaf area. Also, the residual bias is almost eliminated when the big-leaf model is used with the weekly averaged irradiance. This last result appears to favor the use of a big-leaf model for predictions of net photosynthesis on a weekly scale. However, the apparently good fit of the big-leaf model is the result of compensating biases, and might not persist under changing stand conditions. We have shown that the use of a spatially inexplicit multilayer model is possible with the use of scaling variables such as leaf mass per area, in the case of sugar maple.

Acknowledgments

We thank Sébastien Dagnault, Adrien Forgues, Valérie Hudon, Gérard Laroche, Roger Mongrain, Robert Saint-Laurent and René Turcotte for their field assistance. We are grateful to John M. Norman for comments on preliminary versions of the manuscript and to David S. Ellsworth for providing unpublished data on light response of maple. Financial postdoctoral support for F.R. was provided by Natural Resources Canada through the Natural Sciences and Engineering Research Council of Canada.

References

Aber, J.D., P.B. Reich and M.L. Goulden. 1996. Extrapolating leaf CO_2 exchange to the canopy: a generalized model of forest photosynthesis compared with measurements by eddy correlation. Oecologia 106:257–265.

Amthor, J.S., M.L. Goulden, J.W. Munger and S.C. Wofsy. 1994. Testing a mechanistic model of forest-canopy mass and energy exchange using eddy correlation: carbon dioxide and ozone uptake by a mixed oak–maple stand. Aust. J. Plant. Physiol. 21:623–651.

Anonymous. 1982. Canadian climate normals, Vol. 1. Solar radiation 1951–1980. Atmospheric Environment Service, Environment Canada, Ottawa, Canada, 57 p.

Baldocchi, D.D. 1993. Scaling water vapor and carbon dioxide exchange from leaves to a canopy: rules and tools. *In* Scaling Physiological Processes. Leaf to Globe. Eds. J.R. Ehleringer and C.B. Field. Academic Press, San Diego, CA, pp 77–114.

Baldocchi, D.D. and P.C. Harley. 1995. Scaling carbon dioxide and water vapor exchange from leaf to canopy in a deciduous forest. II. Model testing and application. Plant Cell Environ. 18:1157–1173.

Baskerville, G.L. 1972. Use of the logarithmic regression in the estimation of plant biomass. Can. J. For. Res. 2:49–53.

Bates, D.M. and D.G. Watts. 1988. Nonlinear regression analysis and its application. Wiley, New York, 365 p.

Bernier, P.Y., R. Fournier, C.H. Ung, G. Robitaille, G. Larocque, M.B. Lavigne, R. Boutin, F. Raulier, D. Paré, J. Beaubien and C. Delisle. 1999. Linking ecophysiology and forest productivity: an overview of the ECOLEAP project. For. Chron. In press.

Bonan, G.B. 1993. Physiological controls of the carbon balance of boreal forest ecosystems. Can. J. For. Res. 23:1453–1471.

Burger, H. 1939. Baumkrone und Zuwachs in zwei hiebsreifen Fichtenbestanden. Mitt. Schweiz. Anstl. Forstl. Versuchwes. 21:147–175.

Burton, P.J. and F.A. Bazzaz. 1995. Ecophysiological responses of tree seedlings invading different patches of old-field vegetation. J. Ecol. 83:99–112.

Burton, A.J., K.S. Pregitzer and D.D. Reed. 1991. Leaf area and foliar biomass relationships in northern hardwood forests located along an 800 km acid deposition gradient. For. Sci. 37:1041–1059.

Ceulemans, R.J. and B. Saugier. 1991. Photosynthesis. *In* Physiology of Trees. Ed. A.S. Raghavendra. John Wiley & Sons, New York, pp 21–50.

Chen, J.M. and J. Cihlar. 1995. Plant canopy and gap-size theory for improving optical measurements of leaf-area index. Appl. Opt. 34:6211–6222.

Collares-Pereira, M. and A. Rabl. 1979. The average distribution of solar radiation—correlations between diffuse and hemispherical and between daily and hourly insolation values. Sol. Energy 22:155–164.

Collatz, G.J., J.T. Ball, C. Grivet and J.A. Berry. 1991. Physiological and environmental regulation of stomatal conductance, photosynthesis and transpiration: a model that includes a laminar boundary layer. Agric. For. Meteorol. 54:107–136.

Dang, Q.L., H.A. Margolis, M. Sy, M.R. Coyea, G.J. Collatz and C.L. Walthall. 1997. Profiles of photosynthetically active radiation, nitrogen and photosynthetic capacity in the boreal forest: Implications for scaling from leaf to canopy. J. Geophys. Res. 102(D24):28845–28859.

Denholm, J.V. 1981. The influence of penumbra on canopy photosynthesis. I. Theoretical considerations. Agric. Meteorol. 25:167–194.

de Pury, D. and G.D. Farquhar. 1997. Simple scaling of photosynthesis from leaves to canopies without the errors of big-leaf models. Plant Cell Environ. 20:537–557.

Ellsworth, D.S. and P.B. Reich. 1992. Leaf mass per area, nitrogen content and photosynthetic carbon gain in *Acer saccharum* seedlings in contrasting forest light environment. Funct. Ecol. 6:423–435.

Ellsworth, D.S. and P.B. Reich. 1993. Canopy structure and vertical patterns of photosynthesis and related leaf traits in a deciduous forest. Oecologia 96:169–178.

Farquhar, G.D. 1989. Models of integrated photosynthesis and leaves. Phil. Trans. R. Soc. Lond. B 323:357–367.

Farquhar, G.D., S. von Caemmerer and J.A. Berry. 1980. A biochemical model of photosynthetic CO_2 assimilation in leaves of C_3 species. Planta 149:78–90.

Field, C.B. 1983. Allocating leaf nitrogen for the maximization of carbon gain: leaf age as a control on the allocation program. Oecologia 56:341–347.

Gates, D.M. 1980. Biophysical ecology. Springer-Verlag, New York, 611 p.

Givnish, T.J. 1988. Adaptation to sun and shade: a whole plant perspective. Aust. J. Plant. Physiol. 15:63–92.

Goulet, F. and P. Bellefleur. 1986. Leaf morphology plasticity in response to light environment in deciduous tree species and its implication on forest succession. Can. J. For. Res. 16:1192–1195.

Gregoire, T.G., H.T. Valentine and G.M. Furnival. 1995. Sampling methods to estimate foliage and other characteristics of individual trees. Ecology 76:1181–1194.

Hagen, R.H. and J.F. Chabot. 1986. Leaf anatomy of maples (*Acer*) and host use by Lepidoptera larvae. Oikos 47:335–345.

Hanson, P.J., R.E. McRobert, J.G. Isebrands and R.K. Dixon. 1987. An optimal sampling strategy for determining CO_2 exchange rate as a function of photosynthetic photon flux density. Photosynthetica 21:98–101.

Harley, P.C. and D.D. Baldocchi. 1995. Scaling carbon dioxide and water vapour exchange from leaf to canopy in a deciduous forest. I. Leaf model parameterization. Plant Cell Environ. 18:1146–1156.

Harley, P.C., R.B. Thomas, J.F. Reynolds and B.R. Strain. 1992. Modelling photosynthesis of cotton grown in elevated CO_2. Plant Cell Environ. 15:271–282.

Hollinger, D.Y. 1996. Optimality and nitrogen allocation in a tree canopy. Tree Physiol. 16:627–634.

Jarvis, P.G. and J.W. Leverenz. 1983. Productivity of temperate, deciduous and evergreen forests. *In* Physiological Plant Ecology. IV. Encyclopedia of Plant Ecology, Vol. 12D. Eds. O.L. Lange, P.S. Nobel, C.B. Osmond and H. Ziegler. Springer-Verlag, Berlin, pp 234–280.

Jurik, T.W. 1986. Temporal and spatial patterns of specific leaf weight in successional northern hardwood tree species. Am. J. Bot. 73:1083–1092.

Kull, O. and P.G. Jarvis. 1995. The role of nitrogen in a simple scheme to scale up photosynthesis from leaf to canopy. Plant Cell Environ. 18:1174–1182.

Landsberg, J.J. and S.T. Gower. 1997. Applications of physiological ecology to forest management. Academic Press, San Diego, CA, 354 p.

Landsberg, J.J., S.D. Prince, P.G. Jarvis, R.E. McMurtrie, R. Luxmoore and B.E. Medlyn. 1996. Energy conversion and use in forests: An analysis of forest production in terms of radiation utilization efficiency (ε). *In* The Use of Remote Sensing in the Modeling of Forest Productivity. Eds. H.L. Gholz, K. Nakane and H. Shimoda. Kluwer Academic Publishers, Dordrecht, The Netherlands, pp 273–298.

Leuning, R., F.M. Kelliher, D.G.G. de Pury and E.-D. Schulze. 1995. Leaf nitrogen, photosynthesis, conductance and transpiration: scaling from leaves to canopies. Plant Cell Environ. 18:1183–1200.

Liu, X., D.S. Ellsworth and M.T. Tyree. 1997. Leaf nutrition and photosynthetic performance of sugar maple (*Acer saccharum*) in stands with contrasting health conditions. Tree Physiol. 17:169–178.

Lloyd, J., J. Grace, A.C. Miranda, P. Meir, S.C. Wong, H.S. Miranda, I.R. Wright, C. Gash and J. McIntyre. 1995. A simple calibrated model of Amazon rainforest productivity based on leaf biochemical properties. Plant Cell Environ. 18:1129–1145.

McMurtrie, R.E. and Y.-P. Wang. 1993. Mathematical models of the photosynthetic response of tree stands to rising CO_2 concentrations and temperatures. Plant Cell Environ. 16:1–13.

McMurtrie, R.E., H.N. Comins, M.U.F. Kirschbaum and Y.-P. Wang. 1992*a*. Modifying existing forest growth models to take account of effects of elevated CO_2. Aust. J. Bot. 40:657–677.

McMurtrie, R.E., R. Leuning, W.A. Thompson and A.M. Wheeler. 1992*b*. A model of canopy photosynthesis and water use incorporating a mechanistic formulation of leaf CO_2 exchange. For. Ecol. Manag. 52:261–278.

Monsi, M. and T. Saeki. 1953. Über den Lichtfaktor in den Pflanzengesellschaften und seine Bedeutung für die Stoffproduktion. Jpn. J. Bot. 14:22–52.

Niinemets, Ü. and J.D. Tenhunen. 1997. A model separating leaf structural and physiological effects on carbon gain along light gradients for the shade-tolerant species *Acer saccharum*. Plant Cell Environ. 20:845–866.

Nikolov, N.T. and K.F. Zeller. 1992. A solar radiation algorithm for ecosystem dynamic models. Ecol. Model. 61:149–168.

Norman, J.M. 1980. Interfacing leaf and canopy light interception models. *In* Predicting Photosynthesis for Ecosystem Models. Vol. II. Eds. J.D. Hesketh and J.W. Jones. CRC Press, Boca Raton, FL, pp 49–67.

Norman, J.M. 1993. Scaling processes between leaf and canopy levels. *In* Scaling Physiological Processes. Leaf to Globe. Eds. J.R. Ehleringer and C.B. Field. Academic Press, San Diego, CA, pp 41–76.

Norman, J.M. and P.G. Jarvis. 1975. Photosynthesis in Sitka spruce (*Picea sitchensis* (Bong.) Carr.). V. Radiation penetration theory and a test case. J. Appl. Ecol. 12:839–878.

O'Hara, K.L. and K.S. Milner. 1994. Describing forest stand structure: some old and new approaches. Symposium on Mixed Stands. IUFRO Working Group S4.01, 25–29 April 1994, Lousã/Coimbra, Portugal, pp 43–56.

Ouellet, D. 1995. Morphométrie de l'érable à sucre. *In* L'Érable à Sucre, Caractéristiques, Écologie et Aménagement. Ressources naturelles Canada, Ministère des Ressources naturelles Québec et Ministère de l'Agriculture, des Pêcheries et de l'Alimentation, Québec, Canada, pp 29–34.

Powell, G.R., K.J. Tosh and J.E. MacDonald. 1982. Indeterminate shoot extension and heterophylly in *Acer saccharum*. Can. J. For. Res. 12:166–170.

Ratkowsky, D.A. 1990. Handbook of nonlinear regression models. Marcel Dekker, New York, 241 p.

Raulier, F. and C.-H. Ung. 1997. Influence of shading on the relationship between leaf area and crown surface area in sugar maple stands. Ecol. Model. 104:51–69.

Reich, P.B., D.S. Ellsworth, B.D. Kloeppel, J.H. Fownes and S.T. Gower. 1990. Vertical variation in canopy structure and CO_2 exchange of oak–maple forests: influence of ozone, nitrogen, and other factors on simulated canopy carbon gain. Tree Physiol. 7:329–345.

Reich, P.B., B.D. Kloeppel, D.S. Ellsworth and M.B. Walters. 1995. Different photosynthesis-nitrogen relations in deciduous hardwood and evergreen coniferous tree species. Oecologia 104:24–30.

Ross, J. 1975. Radiative transfer in plant communities. *In* Vegetation and the Atmosphere. Vol. 1. Principles. Ed. J.L. Monteith. Academic Press, New York, pp 13–55.

Running, S.W. and J.C. Coughlan. 1988. A general model of forest ecosystem processes for regional applications. I. Hydrological balance, canopy gas exchange and primary productivity processes. Ecol. Model. 42:125–154.

Sellers, W.D. 1965. Physical climatology. The Univ. of Chicago Press, Chicago, IL, 272 p.

Sellers, P.J., J.A. Berry, G.J. Collatz, C.B. Field and F.G. Hall. 1992. Canopy reflectance, photosynthesis and transpiration. III. A reanalysis using improved leaf models and a new canopy integration scheme. Remote Sens. Environ. 42:187–216.

Shinozaki, K., K. Yoda, K. Hozumi and T. Kira. 1964. A quantitative analysis of plant form—the pipe model theory. I. Basic analyses. Jpn. J. Ecol. 14:97–105.

Spitters, C.J.T. 1986. Separating the diffuse and direct component of global radiation and its implications for modeling canopy photosynthesis. Part II. Calculation of canopy photosynthesis. Agric. For. Meteorol. 38:231–242.

Spitters, C.J.T., H.A.J.M. Toussaint and J. Goudriaan. 1986. Separating the diffuse and direct component of global radiation and its implications for modeling canopy photosynthesis. Part I. Components of incoming radiation. Agric. For. Meteorol. 38:217–229.

St-Jacques, C., M. Labrecque and P. Bellefleur. 1991. Plasticity of leaf absorbance in some broadleaf tree seedlings. Bot. Gaz. 152:195–202.

Thibault, M. 1985. Les régions écologiques du Québec méridional, deuxième approximation (map). Ministère de l'Énergie et des Ressources, Québec, Canada.

Thornley, J.H.M. and I.R. Johnson. 1990. Plant and crop modelling. Clarendon Press, Oxford, U.K, 669 p.

Tjoelker, M.G., J.C. Volin, J. Oleksyn and P.B. Reich. 1995. Interaction of ozone pollution and light effects on photosynthesis in a forest canopy experiment. Plant Cell Environ. 18:895–905.

Wang, Y.P. and P.J. Polglase. 1995. Carbon balance in the tundra, boreal forest and humid tropical forest during climate change: scaling up from leaf physiology and soil carbon dynamics. Plant Cell Environ. 18:1226–1244.

West, P.W., D.A. Ratkowsky and A.W. Davis. 1984. Problems of hypothesis testing of regressions with multiple measurements from individual sampling units. For. Ecol. Manag. 7:207–224.

Williams, M., E.B. Rastetter, D.N. Fernandes, M.L. Goulden, S.C. Wofsy, G.R. Shaver, J.M. Melillo, J.W. Munger, S.-M. Fan and K.J. Nadelhoffer. 1996. Modelling the soil-plant atmosphere continuum in a *Quercus–Acer* stand at Harvard Forest: the regulation of stomatal conductance by light, nitrogen and soil/plant hydraulic properties. Plant Cell Environ. 19:911–927.

Wullschleger, S.D. 1993. Biochemical limitations to carbon assimilation in C_3 plants—a retrospective analysis of the A–C_i curves from 109 species. J. Exp. Bot. 44:907–920.

Appendix

The profile of direct irradiance in a canopy can be approximated with the Beer-Lambert model and an expression for its extinction coefficient (e.g., Jarvis and Leverenz 1983, Chen and Cihlar 1995) is:

$$k_b = \Omega\frac{G(\theta)}{\cos\theta}, \tag{A1}$$

where k_b is the extinction coefficient for direct irradiance, Ω is a foliage clumping index, $G(\theta)$ is the mean cosine of the angle defined between the leaves and the sun and θ is the solar zenith angle. We used a value of 0.367 for the product ΩG, derived from the results of Burton et al. (1991), independently of the sun elevation. Burton et al. (1991) estimated a mean value of 0.437 for ΩG when calculating k_b from measured relative irradiances and leaf litter data. This value was multiplied by a factor of 0.84 (± 0.05 SD) because their estimates of LAI calculated from leaf litter data were consistently lower than those estimated with an allometric relationship comparable to Equation 12.

For the diffuse part of irradiance, an average extinction coefficient was estimated assuming an isotropic sky and dividing the sky hemisphere into 10 zenithal angle classes:

$$k_d = -\frac{\ln\left(0.1\sum_{i=1}^{10}\exp(-k_{b_i}L^*)\right)}{L^*}, \tag{A2}$$

where k_{b_i} is the extinction coefficient for direct irradiance in the zenithal angle class i (Equation A1). Because the value of k_d depends of the considered LAI, it was estimated for values of LAI between 2 and 10 in steps of 2.

The algorithm of Collares-Pereira and Rabl (1979) was used to estimate the solar path during the growing season (May 15 to September 15). The terrestrial shortwave radiation model of Nikolov and Zeller (1992) was used to estimate the monthly averaged daily terrestrial radiation on the earth's surface. The model of Collares-Pereira and Rabl (1979, their Equation 10) was then used to estimate the relative importance of diffuse radiation, which depends on day length and a clearness index defined as the ratio between the monthly averaged daily terrestrial and extraterrestrial radiation values. The last model was used instead of that provided by Nikolov and Zeller (1992) because of closest correlation with the diffuse proportion of radiation measured in the Montreal Jean Brébeuf weather station (Anonymous 1982). The PAR was estimated as one half of total shortwave radiation (Ross 1975, Aber et al. 1996).

The growing season was divided into four approximately equal periods with their central class value starting each first day of a month (June, July, August and September). For each central class day, the sun irradiance was estimated every 2 h with a half-sine wave (e.g., Wang and Polglase 1995, their Equation A17). Sun zenith angle was estimated with spherical trigonometry (e.g., Sellers 1965). For each day, the daily PAR radiation below the canopy (H, mol m^{-2} day^{-1}) was estimated for values of LAI between 2 and 10 in steps of 2 as:

$$H = \Delta t\sum_t I_{0.\mathrm{b}}(t)\exp(-k_b L^*) + H_{0.\mathrm{d}}\exp(-k_d L^*), \tag{A3}$$

where Δt (s) is the time separating each estimation of direct beam PAR irradiance above the canopy ($I_{0.\mathrm{b}}$, expressed here in mol m^{-2} s^{-1}) and $H_{0.\mathrm{d}}$ is the monthly averaged daily diffuse PAR radiation (mol m^{-2} day^{-1}) at the top of the canopy. The average extinction coefficient needed for Equations 8 and 10 was then approximated for the whole growing season with:

$$\overline{k} = -\frac{\ln\left(\sum H/\sum H_0\right)}{L^*}, \tag{A4}$$

where H_0 is the total mean monthly daily radiation (mol m^{-2} day^{-1}); *$\overline{k}$ was thus simulated for values of LAI between 2 and 10 in steps of 2. Results were used to adjust the following function from which the $\overline{k}$ for our particular stands were estimated:*

$$\overline{k} = \kappa_1 + \kappa_2\ln(L^*), \tag{A5}$$

where κ_1 and κ_2 are two parameters estimated with OLS. The estimated values are equal to 0.672 (SD of 0.007) for κ_1 and −0.079 (SD of 0.004) for κ_2, with an adjusted coefficient of determination equal to 0.989 and a mean square error of 6.86E−5.